Short Papers

Distributed Equivalent Sources for the Analysis of Multiconductor Transmission Lines Excited by an Electromagnetic Field

ANDREAS C. CANGELLARIS, MEMBER, IEEE

Abstract—**The interaction of multiconductor lines with electromagnetic radiation is commonly studied in terms of field-induced voltage and current sources distributed along the line. This paper presents the relationships between these sources and the incident fields for the general case of a transmission line with its conductors embedded in different dielectric volumes of arbitrary shape. It is shown that the sources can be expressed directly in terms of the incident fields and some vector parameters which are determined from the solution of a series of electrostatic problems with appropriate boundary conditions independent of the incident electric fields.**

I. Introduction

The interaction of multiconductor transmission lines (MTL's) with electromagnetic radiation is usually accounted for through distributed current and voltage sources along the lines, with the current sources being related to the electric field and the voltage sources being proportional to the magnetic field [1], [5]. Fig. 1 shows an array of $N+1$ parallel conductors, the $N+1$ conductor taken as the reference. Each conductor is embedded in an arbitrary volume of homogeneous dielectric medium. Notice that the typical microwave transmission line with N parallel conductors embedded in multiple layers of homogeneous dielectric media above an infinite perfectly conducting plane is a special case of the general configuration of Fig. 1. The MTL is illuminated by an arbitrarily incident plane wave. Under the assumption of lossless lines and quasi-TEM mode of wave propagation, the distribution of voltages and currents along the conductors is described by the following hyperbolic system [5]:

$$\frac{\partial}{\partial z}\boldsymbol{V}(z,t) = -\boldsymbol{L}\frac{\partial}{\partial t}\boldsymbol{I}(z,t) + \boldsymbol{V}_s(z,t) \tag{1a}$$

$$\frac{\partial}{\partial z}\boldsymbol{I}(z,t) = -\boldsymbol{C}\frac{\partial}{\partial t}\boldsymbol{V}(z,t) + \boldsymbol{I}_s(z,t) \tag{1b}$$

where the column vectors $\boldsymbol{V}, \boldsymbol{I}$ are of dimension N and represent the line voltages and currents, respectively. $\boldsymbol{L}, \boldsymbol{C}$ are the $N \times N$ per unit length inductance and capacitance matrices, and $\boldsymbol{V}_s, \boldsymbol{I}_s$ are column vectors of dimension N that incorporate the effect of the external field in the form of distributed voltage and current sources. For an MTL with cross-sectional dimensions small compared to the wavelengths of the exciting EM fields, these voltage and current sources are [3], [5]

$$\boldsymbol{V}_s(z,t) = \begin{pmatrix} \vdots \\ \dfrac{\partial}{\partial t}\displaystyle\int_{C_i} (\vec{B}^{\text{inc}} + \vec{B}^{s}) \cdot \hat{n}\, dl \\ \vdots \end{pmatrix} \tag{2}$$

$$\boldsymbol{I}_s(z,t) = -\boldsymbol{C}\begin{pmatrix} \vdots \\ \dfrac{\partial}{\partial t}\displaystyle\int_{C_i} (\vec{E}^{\text{inc}} + \vec{E}^{s}) \cdot d\vec{l} \\ \vdots \end{pmatrix} \tag{3}$$

where $(\vec{E}^{\text{inc}}, \vec{B}^{\text{inc}})$ are the incident fields, and $(\vec{E}^{s}, \vec{B}^{s})$ are due to the induced quasi-static current and charge distributions on the line, which contribute to the scattered fields but have a net current or charge of zero on each conductor. The integration path C_i appearing in (2), (3) is defined to be a straight line joining the two closest points on the ith and the reference conductor (see Fig. 1).

Before the explicit expressions (2), (3) can be used in (1), it is necessary to evaluate $\vec{E}^{s}$ and $\vec{B}^{s}$ solving an electrostatic and a magnetostatic boundary value problem. In [5], solutions of these problems were given for the case of an MTL in a homogeneous dielectric medium. In what follows, we extend the analysis to the general case of Fig. 1.

II. The Electrostatic Problem

Consider the collection of conductors shown in Fig. 2. They have zero net charge and are embedded in dielectric volumes of permittivity ϵ_i, $i=1,2,\cdots,N+1$. The $N+1$ conductor is taken as reference. In the presence of an incident electric field, a scattered field is produced by the induced charges. The electrostatic potential everywhere in space can be found by solving the following boundary value problem:

$$\nabla^2 \phi_i(\vec{r}) = 0 \qquad (\vec{r} \in V_i); \qquad i = 0,1,\cdots,N+1 \tag{4}$$

$$\phi_i(\vec{r}) = \phi_{0i} \qquad \int_{S_i} \frac{\partial \phi_i(\vec{r})}{\partial n_i}\, dS_i = 0 \qquad (\vec{r} \in S_i); \qquad i = 1,2,\cdots,N+1 \tag{5}$$

$$\epsilon_i \frac{\partial \phi_i(\vec{r})}{\partial n_{di}} = \epsilon_0 \frac{\partial \phi_0(\vec{r})}{\partial n_{di}} \qquad \phi_i(\vec{r}) = \phi_0(\vec{r}) \qquad (\vec{r} \in S_{di}); \qquad i = 1,2,\cdots,N+1 \tag{6}$$

$$\lim_{r \to \infty} \phi_0(\vec{r}) = \phi^{\text{inc}}(\vec{r}) + O\left(\frac{1}{r}\right) = -\vec{r} \cdot \vec{E}^{\text{inc}}(\vec{r}) + O\left(\frac{1}{r}\right) \tag{7}$$

where ϕ_{0i}, $i=1,2,\cdots,N+1$, are the constant potentials on the conductors. Once the potentials of each conductor are de-

Manuscript received October 13, 1987; revised February 4, 1988, and May 9, 1988.

The author was with the Electrical and Electronics Engineering Department, General Motors Research Laboratories, Warren, MI. He is now with the Electromagnetics Laboratory, Department of Electrical and Computer Engineering, University of Arizona, Tucson, AZ 85721

IEEE Log Number 8823089.

0018-9480/88/1000-1445$01.00 ©1988 IEEE

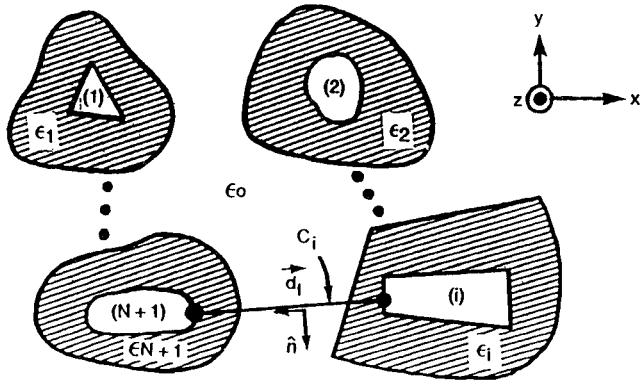

Fig 1 Cross section of a multiconductor transmission line.

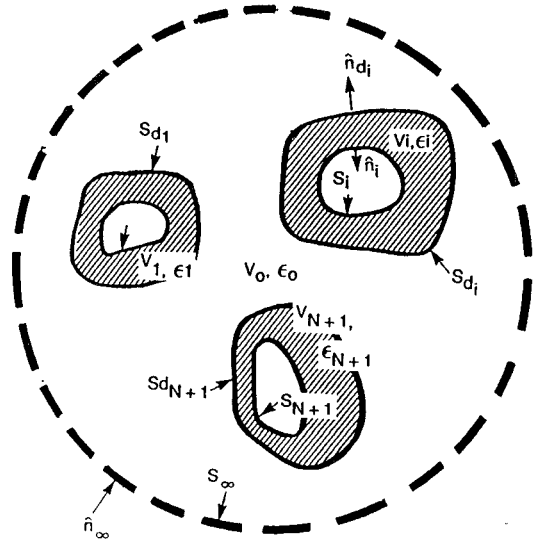

Fig. 2 The geometry for the electrostatic boundary value problem.

termined, the integrals in (3) can be found directly as

$$\int_{C_j} (\vec{E}^{\text{inc}} + \vec{E}^s) \cdot d\vec{l} = -(\phi_{0j} - \phi_{0(N+1)}), \qquad j = 1,2,\cdots,N. \quad (8)$$

It is possible, however, to express the above integral in another form using only the incident field and a vector $\vec{h}_j$ which is a function of the geometry and the electric properties of the line.

Let us consider the following auxiliary problem:

$$\nabla^2 \phi_i^*(\vec{r}) = 0 \qquad (\vec{r} \in V_i); \quad i = 0,1,\cdots,N+1 \quad (9)$$

$$\phi_i^*(\vec{r}) = \phi_{0i}^*, \qquad i = 1,2,\cdots,N+1 \quad (10)$$

$$\int_{S_i} \frac{\partial \phi_i^*(\vec{r})}{\partial n_i} dS_i = 0 \qquad (\vec{r} \in S_i); \quad i = 1,2,\cdots,j-1;\ j+1,\cdots,N \quad (11)$$

$$\epsilon_j \int_{S_j} \frac{\partial \phi_j^*}{\partial n_j} dS_j = -\epsilon_{N+1} \int_{S_{N+1}} \frac{\partial \phi_{N+1}^*}{\partial n_{N+1}} dS_{N+1} = Q_j \quad (12)$$

$$\epsilon_i \frac{\partial \phi_i^*(\vec{r})}{\partial n_{di}} = \epsilon_0 \frac{\partial \phi_0^*(\vec{r})}{\partial n_{di}} \qquad \phi_i^*(\vec{r}) = \phi_0^*(\vec{r}) \qquad (\vec{r} \in S_{di}); \quad i = 1,2,\cdots,N+1 \quad (13)$$

where ϕ_{0i}^*, $i = 1,\cdots,N+1$, are the constant potentials of the conductors. That is, $\phi_i^*(\vec{r})$ are the potentials for the same geometry but with the jth conductor and the reference conductor charged at Q_j and $-Q_j$, respectively. Starting with Green's second identity in the volume V_0 for the potential functions ϕ_0, ϕ_0^* and making use of (4) and (9) for $i = 0$, we have

$$\int_{S_\infty} \left(\phi_0^* \frac{\partial \phi_0}{\partial n_\infty} - \phi_0 \frac{\partial \phi_0^*}{\partial n_\infty} \right) dS_\infty = \sum_{i=1}^{N+1} \int_{S_{di}} \left(\phi_0^* \frac{\partial \phi_0}{\partial n_{di}} - \phi_0 \frac{\partial \phi_0^*}{\partial n_{di}} \right) dS_{di}. \quad (14)$$

Using (6) and (13) we can rewrite (14) as

$$\int_{S_\infty} \left(\phi_0^* \frac{\partial \phi_0}{\partial n_\infty} - \phi_0 \frac{\partial \phi_0^*}{\partial n_\infty} \right) dS_\infty = \sum_{i=1}^{N+1} \frac{\epsilon_i}{\epsilon_0} \int_{S_{di}} \left(\phi_i^* \frac{\partial \phi_i}{\partial n_{di}} - \phi_i \frac{\partial \phi_i^*}{\partial n_{di}} \right) dS_{di}. \quad (15)$$

Applying Green's second identity inside the volume V_i, we get

$$\int_{S_{di}} \left(\phi_i \frac{\partial \phi_i^*}{\partial n_{di}} - \phi_i^* \frac{\partial \phi_i}{\partial n_{di}} \right) dS_{di} = \int_{S_i} \left(\phi_i^* \frac{\partial \phi_i}{\partial n_i} - \phi_i \frac{\partial \phi_i^*}{\partial n_i} \right) dS_i. \quad (16)$$

Using (7) and (16) in (15), we can write

$$\int_{S_\infty} \left(\phi_0^* \frac{\partial \phi^{\text{inc}}}{\partial n_\infty} - \phi^{\text{inc}} \frac{\partial \phi_0^*}{\partial n_\infty} \right) dS_\infty = -\sum_{i=1}^{N+1} \frac{\epsilon_i}{\epsilon_0} \int_{S_i} \left(\phi_i^* \frac{\partial \phi_i}{\partial n_i} - \phi_i \frac{\partial \phi_i^*}{\partial n_i} \right) dS_i. \quad (17)$$

Applying again Green's second identity for ϕ^{inc} and ϕ_0^* inside the volume V_0, and for ϕ^{inc} and ϕ_i^* inside each one of the volumes V_i one gets, after some manipulations,

$$\int_{S_\infty} \left(\phi_0^* \frac{\partial \phi^{\text{inc}}}{\partial n_\infty} - \phi^{\text{inc}} \frac{\partial \phi_0^*}{\partial n_\infty} \right) dS_\infty = \sum_{i=1}^{N+1} \left(\int_{S_i} \frac{1}{\epsilon_i} \phi^{\text{inc}} \sigma_i^* \, dS_i + \int_{S_{di}} \frac{1}{\epsilon_0} \phi^{\text{inc}} \sigma_{\text{pol}(i)}^* \, dS_{di} \right) \quad (18)$$

where the definition for the surface charge density,

$$\sigma_i^* = \epsilon_i \frac{\partial \phi_i^*}{\partial n_i} \quad (19)$$

and the polarization surface charge density for the interface between two dielectrics,

$$\sigma_{\text{pol}(i)}^* = (\epsilon_i - \epsilon_0) \frac{\partial \phi_i^*}{\partial n_{di}} \quad (20)$$

have been used. On the other hand, using (5), (10)–(12), and (19), the right-hand side of (17) becomes

$$-\sum_{i=1}^{N+1} \frac{\epsilon_i}{\epsilon_0} \int_{S_i} \left(\phi_i^* \frac{\partial \phi_i}{\partial n_i} - \phi_i \frac{\partial \phi_i^*}{\partial n_i} \right) dS_i = (\phi_{0j} - \phi_{0(N+1)}) \left(\frac{1}{\epsilon_0} \int_{S_j} \sigma_j^* \, dS_j \right). \quad (21)$$

From (17), (18), and (21) one gets

$$\sum_{i=1}^{N+1} \left(\int_{S_i} \frac{1}{\epsilon_i} \phi^{\text{inc}} \sigma_i^* \, dS_i + \int_{S_{di}} \frac{1}{\epsilon_0} \phi^{\text{inc}} \sigma_{\text{pol}(i)}^* \, dS_{di} \right) = (\phi_{0j} - \phi_{0(N+1)}) \frac{Q_j}{\epsilon_0} \quad (22)$$

or, using the fact that

$$\phi^{\text{inc}} = -\vec{r}\cdot\vec{E}^{\text{inc}} \tag{23}$$

one can finally write

$$-\left(\phi_{0j} - \phi_{0(N+1)}\right) = \vec{E}^{\text{inc}}\cdot\vec{h}_j \tag{24}$$

where

$$\vec{h}_j = \frac{1}{Q_j}\sum_{i=1}^{N+1}\left[\int_{S_i}\left(\frac{\epsilon_0}{\epsilon_i}\right)\vec{r}\sigma_i^*\, dS_i + \int_{S_{di}}\vec{r}\sigma^*_{\text{pol}(i)}\, dS_{di}\right]. \tag{25}$$

Hence, (8) can be conveniently written as

$$\int_{C_j}\left(\vec{E}^{\text{inc}} + \vec{E}^s\right)\cdot d\vec{l} = \vec{E}^{\text{inc}}\cdot\vec{h}_j, \qquad j=1,2,\cdots,N. \tag{26}$$

Physically, $\vec{h}_j$, $j=1,2,\cdots,N$, can be interpreted as the position vectors of the charge centroids of the multiconductor system, given a total charge Q_j on the jth conductor and $-Q_j$ on the reference conductor, all the rest of the conductors having zero net charge. For the homogeneous case ($\epsilon_i = \epsilon_0, \forall i$), $\vec{h}_j$ reduces to the result found in [5]. The solution of these auxiliary electrostatic problems has to be found before the computation of the vectors $\vec{h}_j$, $j=1,2,\cdots,N$, has been completed. An integral equation approach to the solution of such problems can be found in [6]. Whereas the results of [6] are for bare conductors in a homogeneous dielectric, the extension to the inhomogeneous case is straightforward. In addition to the charge distributions on the conductors, the charge distributions on the dielectric interfaces need to be found. The unknown expansion coefficients for these polarization surface charge densities are determined by enforcing the continuity of the normal component of the electric flux density at the dielectric interfaces.

III. The Magnetostatic Problem

For the magnetostatic problem we notice that the presence of the different dielectric media does not have any effect on the solution; therefore, the result is identical to the one in [5], which is repeated here for convenience:

$$\int_{C_j}\left(\vec{B}^{\text{inc}} + \vec{B}^s\right)\cdot\hat{n}\, dl = \left(\vec{h}_j^0\times\hat{z}\right)\cdot\vec{B}^{\text{inc}}, \qquad j=1,2,\cdots,N. \tag{27}$$

Here $\vec{h}_j^0$, $j=1,2,\cdots,N$, are the position vectors found for the homogeneous electrostatic problem ($\epsilon_j = \epsilon_0, \forall j$).

IV. Numerical Example

To demonstrate the applications of the proposed method we consider a nine-wire transmission line above a ground plane excited by a plane wave Gaussian pulse. The line is 1 m long and its conductors are circular wires of radius 1 mm with 0.3 mm dielectric coating of relative dielectric permittivity $\epsilon_r = 2.25$. The conductors are 6 cm above the ground plane and at a distance of 1 cm from each other. At the right end ($z=1$ m) the conductors are terminated at 250 Ω resistors, while at the left end ($z=0$ m) every other conductor is left open starting with the second conductor. The rest of the conductors are also terminated at 250 Ω resistors at their left end. The incident pulse is a Gaussian plane wave $g(t) = A\exp(-t^2/T^2)$ with its electric field vertical to the ground plane. The peak value of the pulse is 5 V/m and its angle of incidence with respect to the z axis is 45° approaching the MTL from the side of the ninth conductor. The value of $T=1$ ns is such that the power content of the incident pulse is negligible for wavelengths less than 0.5 m; therefore our assumptions for cross-sectional dimensions of a line small compared to the wavelength remain valid. The voltage at the right-hand resistor of the first conductor is depicted in Fig. 3. The time step is 0.0667 ns. This should be compared to the induced voltage at the right-end resistor of the second conductor shown in Fig 4. In this case the opening at the left end of the second conductor causes the prolonged multiple reflections which eventually decay due to power dissipation at the resistors.

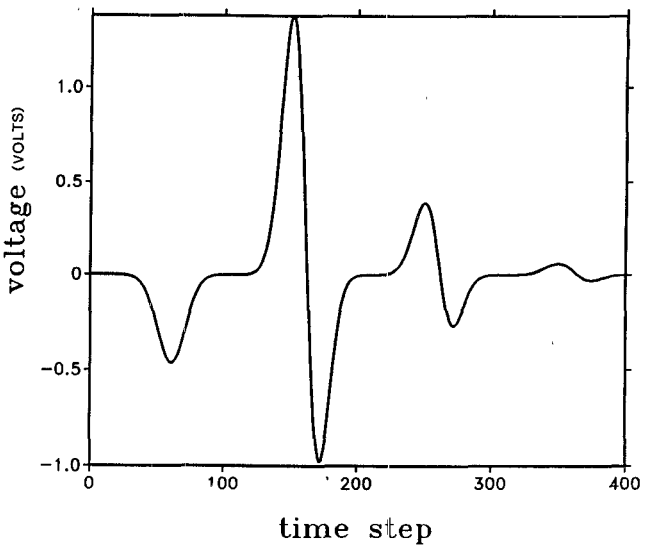

Fig. 3. voltage at the right-end resistor of the first conductor.

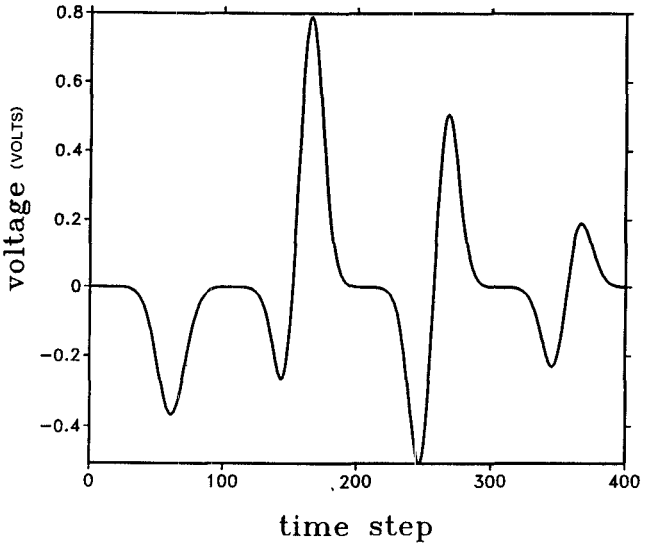

Fig. 4. Voltage at the right-end resistor of the second conductor.

V. Conclusions

Distributed voltage and current sources are commonly used to account for the interaction of electromagnetic radiation with multiconductor transmission lines. This paper has presented the relationships between these sources and the incident fields for the general case where each conductor of the MTL is embedded in an arbitrary volume of a homogeneous dielectric medium. This work generalizes the results of post studies of field excitation of MTL in homogeneous media, making them more suitable for direct applications in microwave transmission lines with rather arbitrary configurations.

REFERENCES

[1] C. D Taylor, R. S. Satterwhite, and C. W Harrison, "The response of a terminated two-wire transmission line excited by a nonuniform electromagnetic field," *IEEE Trans Antennas Propagat.*, vol AP-13, pp 987–989, Nov. 1965.

[2] A. A. Smith, *Coupling of External Electromagnetic Fields to Transmission Lines*. New York: Wiley, 1977

[3] K. S. H. Lee, "Two parallel terminated conductors in external fields," *IEEE Trans. Electromagn Compat*, vol EMC-20, pp 288–296, May 1978

[4] C. R. Paul, "Frequency response of multiconductor transmission lines illuminated by an electric field," *IEEE Trans Electromagn. Compat*, vol EMC-18, pp. 183–186, Nov. 1976.

[5] F. M. Tesche, T. K. Liu, S. K. Chang, and D. V Giri, "Field excitation of multiconductor transmission lines," Air Force Weapons Laboratory Interaction Note 351, Sept. 1978.

[6] D. V. Giri, F. M. Tesche, and S. K. Chang, "A note on the transverse distributions of surface charge densities on multiconductor transmission lines," Air Force Weapons Laboratory Interaction Note 337, Apr 1978

Experimental Studies of the Peak Power-Handling Capacity of Finlines at Centimeter and Millimeter Wavelengths

MICHEL M. NEY, MEMBER, IEEE,
WARREN YUE, STUDENT MEMBER, IEEE, AND
WOLFGANG J. R. HOEFER, SENIOR MEMBER, IEEE

Abstract — **The microwave and millimeter-wave field breakdown in various unilateral finlines is investigated experimentally. First, experiments in the *X*- and *Ka*-band are described to study the breakdown phenomenon and its effects on the structure. Then, experimental values of the maximum transmissible peak power are compared with the theoretical predictions.**

Experimental results confirm the validity of the theoretical model, within a reasonable limit, when the uncertainties produced by the various parameters pertaining to the electric breakdown phenomenon are taken into account.

I. INTRODUCTION

In a recent paper [1], a theoretical model of the electric breakdown phenomenon that occurs in a class of *E*-plane transmission media transmitting pulsed signals was presented. The peak power-handling capacity could be theoretically determined, knowing the geometry and the atmospheric conditions, for frequencies up to 140 GHz. In order to validate the theoretical model, it was necessary to compare the theoretical predictions with measurements.

Unfortunately, very few experimental data are available for *E*-plane structures. Measurements were performed on finline structures (without the waveguide enclosure), in order to verify the accuracy of the finite element method used for field computations [2]. To avoid dissipation and to provide a real quasi-static condition, they were performed at very low frequency. Regarding measurements at higher frequencies, maximum peak power levels for pulsed signals in the *X*-band were recently presented [3]. Unfortunately, no data are available in the *Ka*-band. In the present paper, experiments carried out at 35 GHz (*Ka*-band) are described, the effects of the electric breakdown on the finline structure are examined, and the maximum power that can be transmitted in pulse signal operation is determined. Experimental results in both the *X*- and the *Ka*-band are then discussed and compared with the theoretical predictions.

Manuscript received November 28, 1987; revised April 30, 1988 This work was supported by the Natural Science and Engineering Research Council of Canada.

The authors are with the Department of Electrical Engineering, University of Ottawa, Canada. K1N 6N5.

IEEE Log Number 8823091

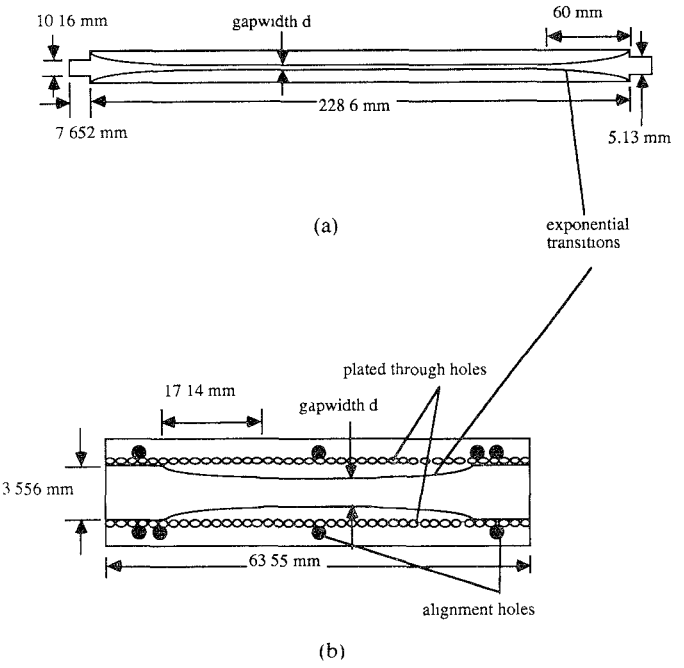

Fig. 1 Finline sample used for experiments at (a) 9 6 GHz and (b) 35.5 GHz.

II. EXPERIMENTAL PROCEDURE

Unilateral finlines with gap widths varying from 0.5 to 2.5 mm and 34 μm metallization thickness were prepared and mounted in a WR-90 waveguide enclosure. For measurements in the *Ka*-band, the gap widths varied from 0.2 to 2 mm, the metallization thickness was 9.9 μm, and the unilateral finlines were mounted in a WR-28 waveguide enclosure. The fins were etched on a 762-μm-thick dielectric substrate (RT/duroid, $\epsilon_r = 2.22$) for the *X*-band measurements. Transitions from finlines to empty waveguide consisted of single exponential tapers. Quarter-wave stubs were cut in the dielectric substrate in order to match it to the empty waveguides (see Fig. 1(a)) [4]. The fins for the *Ka*-band measurements were deposited (plated) on a 254 μm dielectric substrate. Plated holes in the fins prevented leakage to the side ends of the substrate (see Fig. 1(b)).

The block diagram of the measurement system is shown in Fig. 2. A radar station which transmitted a 0.8 μs pulse width signal, with a repetition rate of 1000 pulses/s (0.001 duty cycle) was used for the *X*-band measurement. The generator (magnetron) could produce an adjustable peak power up to a maximum of 300 kW at a fixed frequency of 9.6 GHz. A built-in circulator and a Teflon window prevented damage due to reflections. In order to read the transmitted power level, a power meter calibrated in terms of peak power was connected in front of the test unit. An oscilloscope was connected, through a detector, at the end of the test unit, to observe any sudden change of the signal envelope level which would indicate a breakdown occurrence. For *Ka*-band measurements, the experimental arrangement was the same as for *X*-band measurements, except that a klystron generator was used. Also, the duty cycle was different with a pulse width of 16.6 μs

0018-9480/88/1000-1448$01.00 ©1988 IEEE